920 *Macromolecules* **2010**, *43*, 920–926
DOI: 10.1021/ma9022247

Macromolecules
ARTICLE

# Carbonyl−Phosphine Heteroligation for Pentamethylcyclopentadienyl (Cp*)−Iron Complexes: Highly Active and Versatile Catalysts for Living Radical Polymerization

**Muneki Ishio, Takaya Terashima, Makoto Ouchi,* and Mitsuo Sawamoto***

*Department of Polymer Chemistry, Graduate School of Engineering, Kyoto University, Katsura, Nishikyo-ku, Kyoto 615-8510, Japan*

*Received October 7, 2009; Revised Manuscript Received November 18, 2009*

ABSTRACT: A series of pentamethylcyclopentadienyliron(II) complexes, ligated by one carbonyl (CO) and one phosphine [Cp*Fe(CO)($L^{phos}$)Br; Cp* = $C_5Me_5$; $L^{phos}$ = $PPh_3$, $PMePh_2$, $PMe_2Ph$, P(*m*-tol)$_3$, and P(*p*-tol)$_3$], were employed for living radical polymerization. In conjunction with a bromide initiator [H−(MMA)$_2$−Br], these Cp*Fe complexes catalyzed living radical polymerization of methyl methacrylate (MMA) better controlled than those with the corresponding cyclopentadienyl (Cp) complexes [CpFe(CO)($L^{phos}$)Br; Cp = $C_5H_5$]. The finer control was demonstrated by successful monomer-addition experiments, a wider range of controllable molecular weight ($M_n$ = $10^4$−$10^5$ or $DP_n$ = 100−1000), and narrower molecular weight distributions ($M_w/M_n$ ∼ 1.2). FT-IR analysis of initiator−catalyst model reactions showed that an efficient carbonyl release from the original coordinatively saturated 18e complex into the unsaturated 16e form is important in the catalysis to generate a growing radical from the initiator. The higher catalytic activity allowed controlled polymerizations of other monomers that are not available for the Cp catalysts, such as methyl acrylate and a functional methacrylate with poly(ethylene glycol) pendent group.

## Introduction

Transition-metal-catalyzed living radical polymerization is one of the powerful tools to prepare controlled polymeric architectures for a wide variety of commodity as well as functional monomers (Scheme 1).[1] In this system, a metal catalyst is critical in controlling molecular weight and its distribution, polymerization rate, and versatility in terms of monomers and reaction conditions. The catalyst ($Mt^n$; $n$ = valence number) activates the carbon−halogen bond in an initiator (R−X; X = halogen) or in a dormant polymer terminal (∼∼C−X) via homolytic cleavage to generate a carbon-centered growing radical (R$^\bullet$ or ∼∼C$^\bullet$), while undergoing one-electron oxidation from $Mt^n$ to $Mt^{n+1}$. The radical species are capable of initiating radical propagation, and after some growing steps with monomers, they are capped with the halogen in the oxidized catalyst ($Mt^{n+1}$), thereby to regenerate a dormant species and the original lower valence-state complex ($Mt^n$). Among transition metals, ruthenium (Ru)[2] and copper (Cu)[3] complexes are highly active and induce not only living homopolymerizations but also random and block copolymerizations of many monomers.

Iron complexes offer another class of transition metal catalysts that are increasingly getting important: environmentally benign, safe, less toxic, biocompatible, and abundant.[4] Since the first successful report with $FeCl_2(PPh_3)_2$,[5] the potency of divalent iron ($Fe^{II}$) complexes in living radical polymerization has in fact been demonstrated.[6−19] However, as polymerization catalysts, iron complexes are generally inferior to ruthenium and copper counterparts, especially in terms of versatility and tolerance of polar monomers and solvents.

*Corresponding authors. E-mail: ouchi@living.polym.kyoto-u.ac.jp (M.O.), sawamoto@star.polym.kyoto-u.ac.jp (M.S.).

To overcome these problems, a saturated (18-electron) half-metallocene iron complexes would be promising for active catalysts, if we follow our previous structural design for active ruthenium-based vanguards [e.g., (Ind)RuCl($PPh_3$)$_2$[20] and Cp*RuCl($PPh_3$)$_2$;[21] Ind (indenyl) = $C_9H_7$; Cp* (pentamethylcyclopentadienyl) = $\eta$-$C_5Me_5$], whose metal belongs to group 8 as with iron. The stronger electron donation from the multiple ligands would enhance catalytic activity for the living radical polymerization involving one electron redox. Most importantly, it has been proposed that the saturated "18e" complexes need to turn into unsaturated "16e" forms via a ligand release to accept a halogen on the activation process. The transformation should be one of the most essential processes for superior catalysis or polymerization control.[22]

We thus focused on 18e "heteroligated" cyclopentadienyl iron complexes coordinated with a carbonyl (CO) and a phosphine [CpFe(CO)($L^{phos}$)Br; $L^{phos}$ = phosphine] and expected that either ligand would be selectively and smoothly released on the activation.[23] Because of the coordinatively saturated 18e structure and the robust coordination of a CO ligand, these catalysts indeed turned out to be highly active in living radical polymerization of methyl methacrylates (MMA) and, when isolated, to be so stable as to be handled even under air at room temperature. Once they encounter an initiator (R−Br) at 60 °C, however, they immediately and irreversibly release the CO ligand to generate *in situ* a real active catalyst [CpFe($L^{phos}$)Br] that is active enough to induce living radical polymerization of MMA. However, their catalytic activity is insufficient to polymerize acrylates and polar functional methacrylates.

In this work, therefore, we designed pentamethylcyclopentadienyliron(II) complexes [Cp*$Fe^{II}$(CO)($L^{phos}$)Br] with a similar carbonyl−phosphine heteroligation toward further improvement of the Cp−iron catalyst family, i.e., to be more active, easier

 Published on Web 12/03/2009 

**Scheme 1**

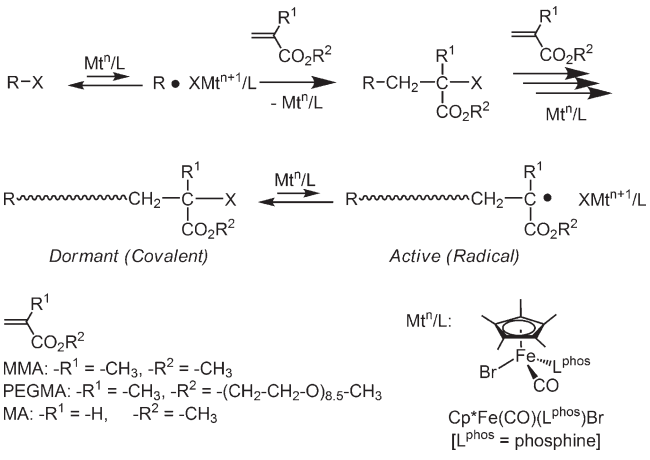


**Scheme 2**

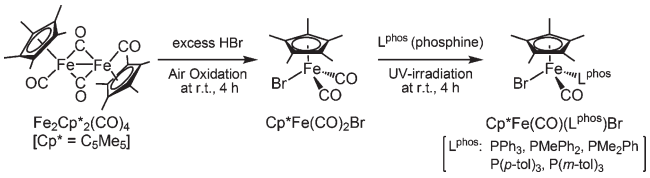


to handle, and more versatile and tolerant of functional monomers. The design is in part based on ruthenium complexes that the high electron ability of Cp* ligand enhances catalytic activity.[21,24] Thus, a series of Cp*Fe(CO)($L^{phos}$)Br were prepared by the reactions of Cp*Fe(CO)$_2$Br with phosphine under UV-irradiation (Scheme 2).[25] They accordingly showed better catalytic performances in MMA polymerization than the CpFe catalysts in terms of molecular weight control and sustained activity (up to >90% conversion). More importantly, some Cp* complexes gave controlled polymers even from methyl acrylate (MA) and a methacrylate (PEGMA) carrying a poly(ethylene glycol) pendent group.

## Experimental Section

**Materials.** MMA (TCI; purity >99%) was dried overnight over calcium chloride and purified by double distillation from calcium hydride before use. MA (TCI; purity >99%) was dried overnight over calcium chloride and purified by distillation from calcium hydride before use. Poly(ethylene glycol) methyl methacrylate [PEGMA; $CH_2{=}CMeCO_2(CH_2CH_2O)_nMe$; Me = $CH_3$; $n$ = 8.5 on average] (Aldrich) and *N,N′*-dimethylaminoethyl methacrylate (DMAEMA) (TCI; purity >98%) were of commercial source and purified by passing through an inhibitor removal column (Aldrich) and degassed by reduced pressure before use.

The MMA dimer bromide [H−(MMA)$_2$−Br; H−(CH$_2$-CMeCO$_2$Me)$_2$−Br] as an initiator was prepared according to the literature.[26] $Cp_2Fe_2(CO)_4$ (Aldrich; purity >99%) and $Cp^*_2Fe_2(CO)_4$ (Azmax; purity >98%) were used as received and handled in a glovebox (M. Braun Labmaster 130) under a moisture- and oxygen-free argon atmosphere ($H_2O$ < 1 ppm; $O_2$ < 1 ppm). Triphenylphosphine ($PPh_3$: Aldrich, purity >99%), methyldiphenylphosphine ($PMePh_2$: Aldrich, purity >99%), dimethylphenylphosphine ($PMe_2Ph$: Aldrich, purity >97%), tri-*p*-tolylphosphine [P(*p*-tol)$_3$: Wako, purity >98%], and tri-*m*-tolylphosphine [P(*m*-tol)$_3$: Aldrich, purity >97%] were used as received.

Toluene, THF, $CH_2Cl_2$, and *n*-hexane (Kishida Kagaku; purity >99%) were passed through purification columns (Solvent Dispensing System; Glass Contour) and bubbled with dry nitrogen for more than 15 min immediately before use. $CHCl_3$ (Wako Chemicals, anhydrous; purity >99%) was bubbled with dry nitrogen for more than 15 min immediately before use. Cyclohexane (Wako, anhydrous) was used as received. *n*-Octane (internal standard for gas chromatography) and 1,2,3,4-tetrahydronaphthalene (tetralin; internal standard for $^1$H NMR analysis) were dried over calcium chloride and distilled twice from calcium hydride.

**Catalyst Synthesis.** CpFe(CO)$_2$Br[27] and CpFe(CO)(PMePh$_2$)Br[28] were synthesized according to the literature. Cp*Fe(CO)$_2$Br was synthesized by the method of King et al.[29] IR ($CHCl_3$): 2028, 1979 cm$^{-1}$ $\nu$(CO). Anal. Calcd for $C_{12}H_{15}BrFeO_2$: C, 44.08; H, 4.62; Br, 24.44. Found: C, 44.31; H, 4.45; Br, 24.65.

A series of Cp*Fe(CO)($L^{phos}$)Br were synthesized by the method of Barras et al. as follows:[25] A cyclohexane (100 mL) and THF (7.0 mL) mixed solution of Cp*Fe(CO)$_2$Br (1.0 g, 3.06 mmol) and 1.5 equiv of phosphine [$L^{phos}$ = $PPh_3$, $PMePh_2$, $PMe_2Ph$, P(*m*-tol)$_3$, or P(*p*-tol)$_3$] was magnetically stirred and was irradiated under UV (Riko, UVL-400P; 400 W) at 25 °C for 4 h under dry argon. The solutions changed from rust to green irrespective of phosphine employed. The reaction mixture was evaporated, and then the residue was washed with *n*-hexane (15 mL × 2). The residue was extracted in toluene (60 mL) and filtered at 25 °C to remove precipitates, and the filtrate was evaporated in vacuo to dryness to remove the solvent. The crude product was dissolved in $CH_2Cl_2$ (7.0 mL) and recrystallized by gradual addition of *n*-hexane (60 mL), followed by standing at −30 °C for 72 h. The supernatant solvent were removed by a cannula with filter paper, and the crystal was washed with *n*-hexane (2.0 mL × 2) and dried under vacuum. The complexes were characterized by elemental analysis, IR spectroscopy at room temperature in $CHCl_3$ on a JASCO FT/IR 4200, and 500 MHz $^1$H NMR spectroscopy at room temperature in $CDCl_3$ on a Jeol JNM-ECA500 spectrometer.

Cp*Fe(CO)($PPh_3$)Br: isolated yield, 75%. $^1$H NMR (ppm): 1.3−1.5 (m, 15H, Cp−C$H_3$), 7.3−7.6 (m, 15H, Ar−*H*). IR ($CHCl_3$): 1931 cm$^{-1}$ $\nu$(CO). Anal. Calcd for $C_{29}H_{30}BrFeOP$: C, 62.06; H, 5.39; Br, 14.24. Found: C, 62.04; H, 5.32; Br, 14.31.

Cp*Fe(CO)($PMePh_2$)Br: isolated yield, 35%. $^1$H NMR (ppm): 1.4−1.6 (m, 15H, Cp−C$H_3$), 2.00 (d, 3H, P−C$H_3$), 7.4−7.8 (m, 10H, Ar−*H*). IR ($CHCl_3$): 1928 cm$^{-1}$ $\nu$(CO). Anal. Calcd for $C_{24}H_{28}BrFeOP$: C, 57.74; H, 5.65; Br, 16.01. Found: C, 57.74; H, 5.54; Br, 16.14.

Cp*Fe(CO)($PMe_2Ph$)Br: isolated yield, 72%. $^1$H NMR (ppm): 1.4−1.5 (m, 15H, Cp−C$H_3$), 1.60 (d, 3H, P−C$H_3$), 1.86 (d, 3H, P−C$H_3$), 7.4−7.7 (m, 5H, Ar−*H*). IR ($CHCl_3$): 1925 cm$^{-1}$ $\nu$(CO). Anal. Calcd for $C_{19}H_{26}BrFeOP$: C, 52.20; H, 6.00; Br, 18.28. Found: C, 52.01; H, 5.93; Br, 18.03.

Cp*Fe(CO)[P(*m*-tol)$_3$]Br: isolated yield, 70%. $^1$H NMR (ppm): 1.3−1.5 (m, 15H, Cp−C$H_3$), 2.29 (m, 9H, Ph−C$H_3$), 7.1−7.3 (m, 12H, Ar−*H*). IR ($CHCl_3$): 1931 cm$^{-1}$ $\nu$(CO). Anal. Calcd for $C_{32}H_{36}BrFeOP$: C, 63.70; H, 6.01; Br, 13.24. Found: C, 64.56; H, 5.95; Br, 12.58.

Cp*Fe(CO)[P(*p*-tol)$_3$]Br: isolated yield, 67%. $^1$H NMR (ppm): 1.2−1.3 (m, 15H, Cp−C$H_3$), 2.31 (m, 9H, Ph−C$H_3$), 7.1−7.4 (m, 12H, Ar−*H*). IR ($CHCl_3$): 1930 cm$^{-1}$ $\nu$(CO). Anal. Calcd for $C_{32}H_{36}BrFeOP$: C, 63.70; H, 6.01; Br, 13.24. Found: C, 62.57; H, 5.84; Br, 16.11.

**Polymerization Procedures.** Polymerization was carried out by the syringe technique under dry argon in baked glass tubes equipped with a three-way stopcock or in sealed glass vials. A typical procedure for MMA polymerization with H−(MMA)$_2$−Br/Cp*Fe(CO)($PMePh_2$)Br was as follows. In a 50 mL round-bottom flask Cp*Fe(CO)($PMePh_2$)Br (25.0 mg, 0.05 mmol), toluene (2.23 mL), *n*-octane (0.27 mL), MMA (2.14 mL, 20 mmol), and H−(MMA)$_2$−Br (0.36 mL of 553.4 mM in toluene, 0.20 mmol) were added sequentially under dry argon at room temperature where the total volume of reaction mixture was thus 5.0 mL. Immediately after mixing, aliquots (0.80 mL

each) of the solution were injected into glass tubes which were then sealed (except when a stopcock was used) and placed in an oil bath kept at desired temperature. In predetermined intervals, the polymerization was terminated by cooling the reaction mixtures to −78 °C. Monomer conversion was determined from the concentration of residual monomer measured by gas chromatography with *n*-octane as an internal standard. The quenched reaction solutions were diluted with toluene (ca. 20 mL), washed with water three times, and evaporated to dryness to give the products that were subsequently dried overnight under vacuum at room temperature.

For MA, the same procedures as descried above were applied, and for PEGMA, the same procedures as described above were applied except that monomer conversion was determined by $^1$H NMR from the integrated peak area of the olefinic protons of the monomers with tetralin as internal standard. The products were similarly isolated but without washing with water because of their hydrophilicity.

**Measurements.** For poly(MMA) and poly(MA), $M_n$ and $M_w/M_n$ were measured by size-exclusion chromatography (SEC) in chloroform at 40 °C on three polystyrene gel columns [Shodex K-805 L (pore size: 20−1000 A; 8.0 mm i.d. × 30 cm); flow rate, 1.0 mL/min] connected to a Jasco PU-980 precision pump, a Jasco 930-RI refractive index detector, and a Jasco 970-UV ultraviolet detector. The columns were calibrated against 13 standard poly(MMA) samples (Polymer Laboratories; $M_n$ = 630−1 200 000, $M_w/M_n$ = 1.06−1.22) as well as the monomer. For poly(PEGMA), DMF containing 10 mM LiBr was applied as an eluent.

Cyclic voltammograms were recorded by using a Hokuto Denko HZ-3000 apparatus. A typical procedure is as follows: Cp*Fe(CO)($PMePh_2$)Br (17.5 mg, 0.035 mmol) was dissolved into a 100 mM solution of *n*-$Bu_4NPF_6$ (supporting electrolyte) in $CH_2Cl$-$CH_2Cl$ (7.0 mL) under dry argon in a baked glass tube equipped with a three-way stopcock. Voltammograms were recorded under argon at a scan rate 0.1 V $s^{-1}$ in a three-electrode cell equipped with a platinum disk as a working electrode, a platinum wire as a counter electrode, and an Ag/AgCl electrode as a reference.

FT-IR spectra of the Cp*Fe complexes were recorded by using a JASCO FT/IR 4200. The sample was prepared that Cp*Fe(CO)($PMePh_2$)Br (2.5 mg, 5.0 × $10^{-3}$ mmol), H−$(MMA)_2$−Br (5.6 mg, 0.020 mmol), and toluene (1.0 mL) were added into the baked glass tube equipped with a three-way stopcock under dry argon. After mixing at 60 °C for 8 h, the solvent was evaporated. The residue was dissolved in degassed $CHCl_3$ and purged in the sealed liquid KBr cell where the thickness was 0.1 mm. Measurements were carried out under an inert atmosphere.

## Results and Discussion

**Ligand Effects on the Catalytic Performance of Cp*Fe(CO)($L^{phos}$)Br.** To investigate the effects of the phosphine ligands in heteroligation, we first employed a series of Cp*Fe(CO)($L^{phos}$)Br [$L^{phos}$ = $PPh_3$, $PMePh_2$, $PMe_2Ph$, P(*m*-tol)$_3$, and P(*p*-tol)$_3$] and their common dicarbonyl precursor [Cp*Fe$(CO)_2$Br] for living radical polymerization of MMA in toluene at 60 °C ($[MMA]_0/[H-(MMA)_2-Br]_0$/[iron complex]$_0$ = 4000/40/10 mM) (Figure 1). All the heteroligated complexes induced smooth polymerization, and monomer conversion reached over 90% within 48 h (Figure 1A). The molecular weights of the obtained PMMAs were increased in direct proportion to monomer conversion and were close to the calculated values assuming that one initiator produced one polymer chain (Figure 1B). After the polymerizations, the brown color, derived from the catalyst, was disappeared to be transparent by water washing, indicating "catalyst removal" possible. On the other hand, the dicarbonyl version resulted in a slower polymerization, a limited conversion (∼50%), and poorly controlled molecular weight

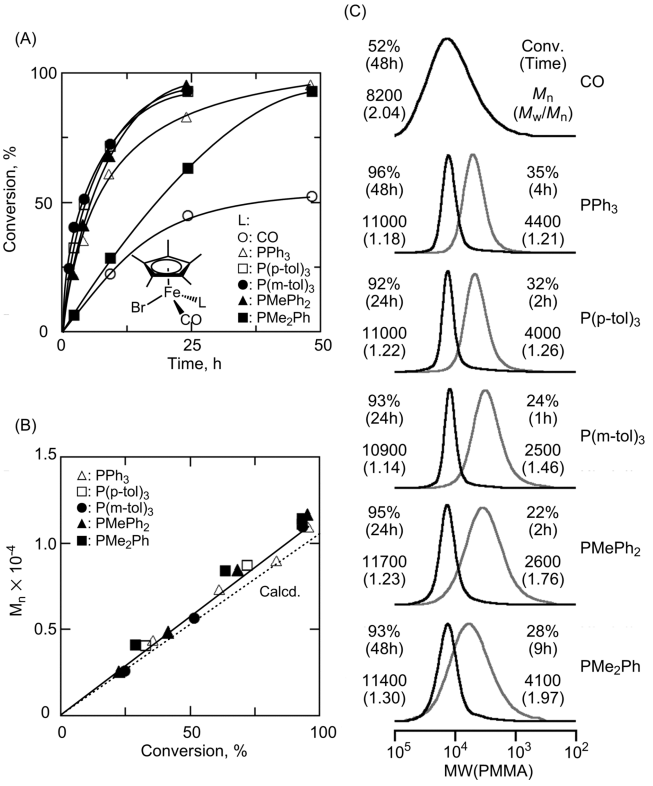


**Figure 1.** Ligand effects of Cp*Fe(CO)($L^{phos}$)Br on living radical polymerization of MMA with H−$(MMA)_2$−Br in toluene at 60 °C: $[MMA]_0$ = 4000 mM; $[H-(MMA)_2-Br]_0$ = 40 mM; [Cp*Fe(CO)($L^{phos}$)Br]$_0$ = 10 mM. Ligand: CO (○); $PPh_3$ (△); P(*p*-tol)$_3$ (□); P(*m*-tol)$_3$ (●); $PMePh_2$(▲); $PMe_2Ph$ (■). (A) Time−conversion plots. (B) Conversion−$M_n$ plots. (C) SEC curves.

distributions (MWDs; $M_w/M_n$ > 2). In this case, the catalyst color was not disappeared via the water-washing procedure after the polymerization. Thus, the heteroligated complexes were more active and better catalysts.

Within the Cp*Fe family, polymerization rate was dependent on the phosphine ligands: P(*p*-tol)$_3$ ≈ P(*m*-tol)$_3$ ≈ $PMePh_2$ > $PPh_3$ > $PMe_2Ph$. This would be linked to the structural conversion of the saturated 18e complex into the corresponding unsaturated 16e variant upon the halogen abstraction from the dormant carbon−halogen terminal, as demonstrated for CpFe(CO)($L^{phos}$)Br.[23]

**Model Reactions with Dormant End Model.** Thus, model reactions of the Cp*Fe catalysts with the initiator [H−$(MMA)_2$−Br] at the polymerization temperature (60 °C) were analyzed by monitoring changes in the carbonyl ligands by FT-IR; H−$(MMA)_2$−Br was considered as the smallest homologue of the dormant PMMA species capped with bromine. Figure 2 shows IR spectra (1600−2200 $cm^{-1}$ region) of a catalyst−initiator equimolar mixture before (upper) and after (down) the reactions. The peaks at around 1900−2000 $cm^{-1}$ are derived from the C≡O stretching of the ligand and those around 1730 $cm^{-1}$ from the ester C═O in the initiator.

Notably, upon mixing with the dormant model, the carbonyl signals of all Cp*Fe(CO)($L^{phos}$)Br catalysts but the $PMe_2Ph$ derivative almost disappeared (Figure 2A−D), suggesting conversion of the saturated and heteroligated 18e complexes into carbonyl-free unsaturated 16e complexes Cp*Fe($L^{phos}$)Br.

The same model systems were also analyzed by $^{31}$P NMR spectroscopy to see the phosphine coordination status. Even after mixing with the dormant model, the signals of the phosphine ligands remained unchanged regardless of the

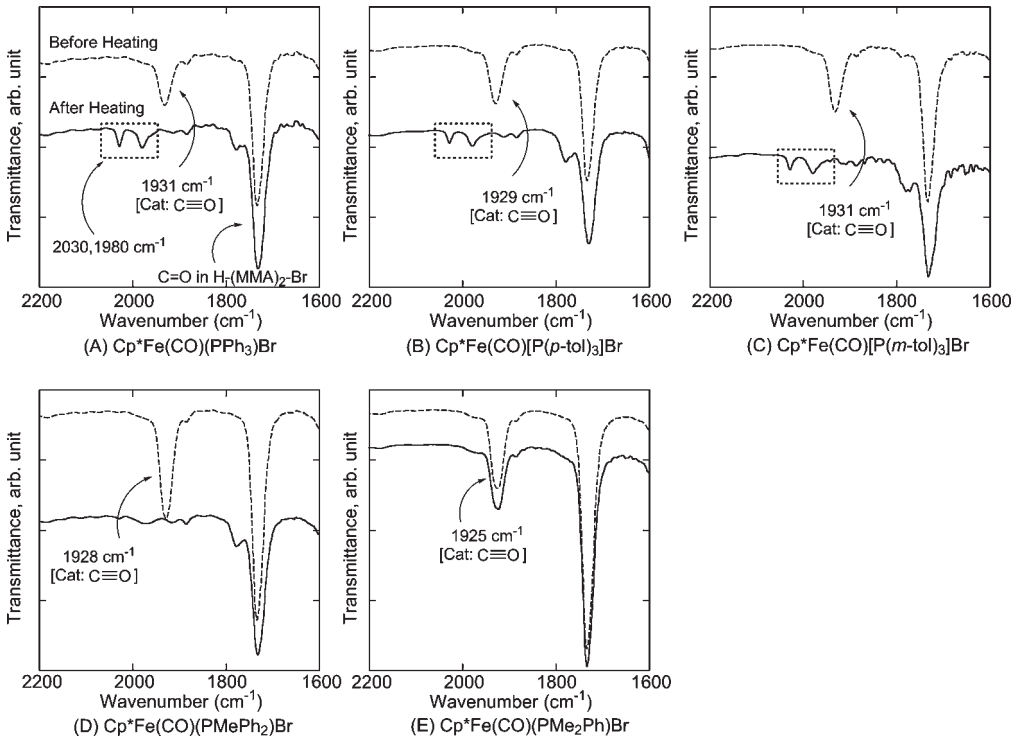


**Figure 2.** IR analysis of Cp*Fe(CO)($L^{phos}$)Br/H−$(MMA)_2$−Br in $CHCl_3$ at 25 °C: [Cp*Fe(CO)($L^{phos}$)Br]$_0$ = 5.0 mM; [H−$(MMA)_2$−Br]$_0$ = 20 mM. Condition: "before heating" (gray line); "after heating", aged at 60 °C for 8 h before measurement (solid line). Cp*Fe(CO)($L^{phos}$)Br: (A) Cp*Fe(CO)($PPh_3$)Br; (B) Cp*Fe(CO)[P(*p*-tol)$_3$]Br; (C) Cp*Fe(CO)[P(*m*-tol)$_3$]Br; (D) Cp*Fe(CO)($PMePh_2$)Br; (E) Cp*Fe(CO)($PMe_2Ph$)Br.

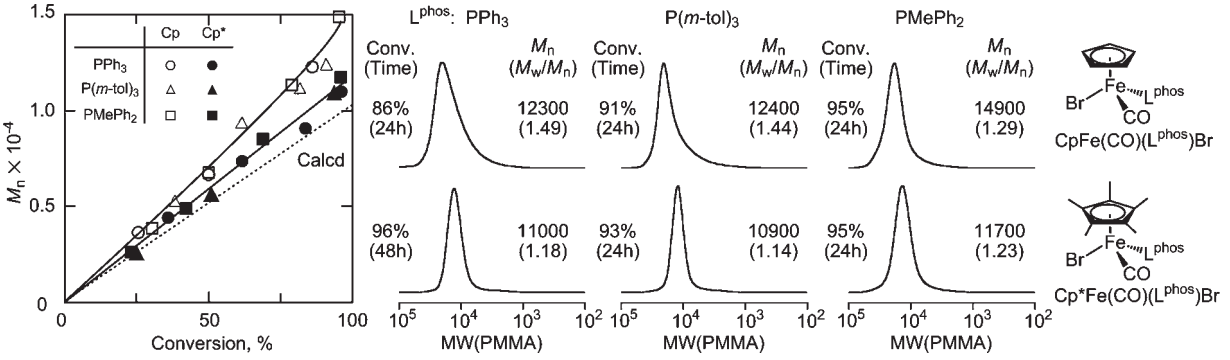


**Figure 3.** Comparisons between CpFe(CO)($L^{phos}$)Br and Cp*FeBr(CO)($L^{phos}$)Br on living radical polymerization of MMA with H−$(MMA)_2$−Br in toluene at 60 °C: [MMA]$_0$ = 4000 mM; [H−$(MMA)_2$−Br]$_0$ = 40 mM; [iron catalyst]$_0$ = 10 mM. Iron catalyst: CpFe(CO)($PPh_3$)Br (○); CpFe(CO)-[P(*m*-tol)$_3$]Br (△); CpFe(CO)($PMePh_2$)Br (□); Cp*Fe(CO)($PPh_3$)Br (●); Cp*Fe(CO)[P(*m*-tol)$_3$]Br (▲); Cp*Fe(CO)($PMePh_2$)Br (■).

phosphine structures, and no peaks indicative of free phosphines were observed, either, all excluding the possible phosphine rather than carbonyl elimination.

With a vacant site for halogen extraction from the dormant end (∼∼C−Br) now available, the 16e complexes would be real "active" catalysts for living radical polymerization, as recently observed with CpFe(CO)($L^{phos}$)Br catalysts.[23] Comparison with similar model reactions for the CpFe family indicates that the 18e−16e conversion apparently occurs faster with the Cp*Fe derivatives, which accounts for the faster polymerizations and the narrower MWDs with these catalysts.

In contrast, the C≡O peak for the $PMe_2Ph$ complex obviously remained intact after the reaction (Figure 2E), suggesting a slow carbonyl release and thereby a slow transformation into the 16e complex. This is consistent with the slower polymerization and the broader MWDs (especially at the initial stage) observed with this catalyst (Figure 1A,C).

Specifically for the triphenylphosphine-based complexes [$L^{phos}$ = $PPh_3$, P(*p*-tol)$_3$, P(*m*-tol)$_3$], two minor peaks newly emerged at higher wave numbers (1980 and 2030 $cm^{-1}$) upon the disappearance of the carbonyl 1900−2000 $cm^{-1}$ bands, and the positions of the new signals were exactly the same as for the dicarbonyl complex [Cp*Fe(CO)$_2$Br] (Figure 2A−C). Such byproduct did not form from similar CpFe complexes or from Cp*Fe(CO)($PMePh_2$)Br. Given the poor catalytic performance of the dicarbonyl complex (see above and Figure 1), however, the real active catalysts should be the in situ formed carbonyl-free 16e complexes [Cp*Fe($L^{phos}$)Br]. The role of the dicarbonyl complex is under investigation, but it might contribute to the deactivation process (radical−halogen coupling) because the polymer MWDs at the final conversions were obviously narrower than that with Cp*Fe(CO)($PMePh_2$)Br, which did not give the dicarbonyl complex.

**Comparison with Cp-Based Complexes.** Let us focus on the difference between the Cp- and the Cp*-based complexes [(Z)Fe(CO)($L^{phos}$)Br; *Z* = Cp, Cp*] in the catalysis for MMA polymerization. Figure 3 shows conversion−$M_n$ plots and SEC curves at around 90% conversion for the

**Table 1. Cyclic Voltammetry Analyses of CpFe(CO)($L^{phos}$)Br and Cp*Fe(CO)($L^{phos}$)Br[a]**

| ligand | | $E_{pa}$ (V) | $E_{pc}$ (V) | $E_{1/2}$ (V) | $\Delta E$ (V) |
|---|---|---|---|---|---|
| $PPh_3$ | Cp | 0.90 | 0.72 | 0.81 | 0.18 |
| | Cp* | 0.63 | 0.46 | 0.55 | 0.18 |
| P(*m*-tol)$_3$ | Cp | 0.83 | 0.65 | 0.74 | 0.18 |
| | Cp* | 0.62 | 0.40 | 0.51 | 0.22 |
| $PMePh_2$ | Cp | 0.88 | 0.71 | 0.79 | 0.17 |
| | Cp* | 0.63 | 0.44 | 0.53 | 0.19 |

[a] [Iron complex]$_0$ = 5 mM, [*n*-$Bu_4NPF_6$]$_0$ = 100 mM in $CH_2ClCH_2Cl$ at 25 °C. $E_{1/2} = (E_{pa} + E_{pc})/2$, $\Delta E = E_{pa} - E_{pc}$.

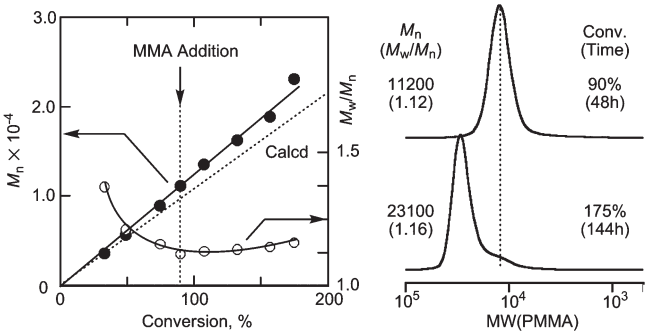


**Figure 4.** Monomer-addition experiment in the polymerization of MMA with H−(MMA)$_2$−Br/Cp*Fe(CO)[P(*m*-tol)$_3$]Br in toluene at 60 °C: [MMA]$_0$ = [MMA]$_{add}$ = 4000 mM; [H−(MMA)$_2$−Br]$_0$ = 40 mM; [Cp*Fe(CO)[P(*m*-tol)$_3$]Br]$_0$ = 4.0 mM.

polymerizations with both catalyst series carrying $PPh_3$, P(*m*-tol)$_3$, and $PMePh_2$. There was little difference in overall polymerization rate (i.e., time to reach ~90% conversion) between the two categories with the same phosphine ligand. On the other hand, polymer MWDs were obviously narrower, and molecular weights better controlled (closer to the calculated), for the Cp* complexes, especially with $PPh_3$ and P(*m*-tol)$_3$. From these results, the Cp* complexes catalyzed a faster reversible activation between dormant and active species with a higher initiating efficiency.

The contribution of Cp* as a conjugated electron-donating group was indeed supported by the lower redox potentials measured by cyclic voltammetry (CV) (Table 1). The half-wave oxidation potentials ($E_{1/2}$) are invariably lower for Cp* by > 0.2 V for three phosphine ligands. Within the Cp or Cp* families, the oxidation potential also depended on the phosphine ligands, and the observed order $PPh_3$ > $PMePh_2$ > P(*m*-tol)$_3$, though not very significant, agrees with the rate order in MMA polymerization (see above and Figure 1).

**High Catalytic Activity and Controllability.** To demonstrate the high catalytic activity and controllability of Cp*Fe(CO)($L^{phos}$)Br, we performed a monomer-addition experiment with the *m*-tolyl−phosphine complex [$L^{phos}$ = P(*m*-tol)$_3$]. When a conversion reached around 90% in the polymerization of MMA, a fresh MMA was added to the polymerization solution. Even in the second phase, MMA was smoothly consumed to give an additional 85% conversion (total 175% relative to the first feed) (Figure 4). Beyond the second monomer addition, molecular weight increased in direct proportion with conversion, and the SEC (MWD) curves shifted to higher molecular weight keeping narrow distributions ($M_w/M_n$ = 1.16), although a slight tailing was detected. As a concurrent addition of the catalyst was not required, the catalytic activity seemed to be kept during the second-stage polymerization.

The high catalytic activity of Cp*Fe(CO)[P(*m*-tol)$_3$]Br encouraged us to synthesize higher molecular weight polymers with narrow MWDs. We thus varied the monomer/initiator feed ratio from 100 through 400 to 1000, targeting $M_n$ up to $10^5$ at 100% conversion (Figure 5). Under all these conditions, conversion reached over 90%, and the molecular weights invariably agreed well with the calculated values based on the feed ratio and conversion, keeping fairly narrow MWDs ($M_w/M_n$ < 1.4). These results demonstrate a high catalytic activity or a high turnover frequency of the Cp*Fe catalyst.

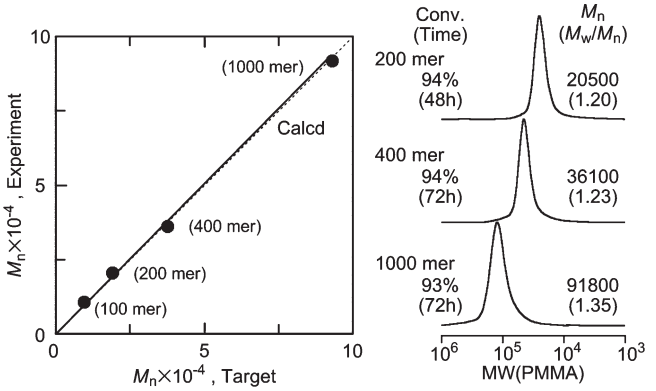


**Figure 5.** Synthesis of high molecular weight PMMA targeted 100-mer (A), 200-mer (B), 400-mer (C), and 1000-mer (D) with H−(MMA)$_2$−Br/Cp*Fe(CO)[P(*m*-tol)$_3$]Br in toluene at 60 °C: [MMA]$_0$/[H−(MMA)$_2$−Br]$_0$/[Cp*Fe(CO)[P(*m*-tol)$_3$]Br]$_0$ = 4000/40/10 mM (A), 4000/20/4.0 mM (B), 4000/10/2.0 mM (C), and 5000/5.0/1.0 mM (D).

**Polymerization of Functional Monomers.** The higher catalytic activity of the Cp* catalysts also promised application for other monomers, especially functional monomers. We then addressed a polymerization of a methacrylate (PEGMA) carrying a poly(ethylene glycol) pendant, one of the popular functional monomers. Figure 6 shows a comparison of the PEGMA polymerizations with Cp*Fe(CO)(PMe$Ph_2$)Br and CpFe(CO)(PMe$Ph_2$)Br. The Cp catalyst gave a decelerated polymerization with a limited conversion (~70%), whereas the Cp* derivative induced an almost quantitative polymerization (conversion >90%). Moreover, the latter produced better-controlled polymers with narrower MWDs [$M_w/M_n$ = 1.29 (Cp*) vs 1.51 (Cp)]. Thus, the enhancement of electron density by the Cp* ligand was found to improve catalytic activity for a functional monomer.

However, this catalyst was still insufficient for an amine-containing monomer, *N,N*′-dimethylaminoethyl methacrylate (DMAEMA), for which polymer MWD was much broader, though conversion reached high (>90%) in 25 h. The interaction of the amino moiety with the catalyst would disrupt the equilibrium balance between dormant and active species. Further ligand design is required for such functional monomers with higher polarity and coordinating nature.

Given the catalytic activity of Cp*Fe(CO)(PMe$Ph_2$)Br for PEGMA, a sequential block copolymerization of MMA and PEGMA was performed with H−(MMA)$_2$−Br (Figure 7). MMA (100 equiv to initiator) was first polymerized in conjunction in toluene at 60 °C. When MMA conversion reached 80% in 25 h, PEGMA (50 equiv) and an additional feed of the catalyst (2.0 mM) were added into the reaction mixture. The added PEGMA was smoothly consumed, and its conversion reached around 80% within 48 h (total 72 h). SEC curves shifted to higher molecular weight, indicative of long-lived growing species, but small shoulders were seen on both sides of the main peak, probably due to dead and coupling polymers.

**Polymerization of MA.** As reported in our previous paper, a heteroligated Cp-based complex [CpFe(CO)(PMe$Ph_2$)Br]

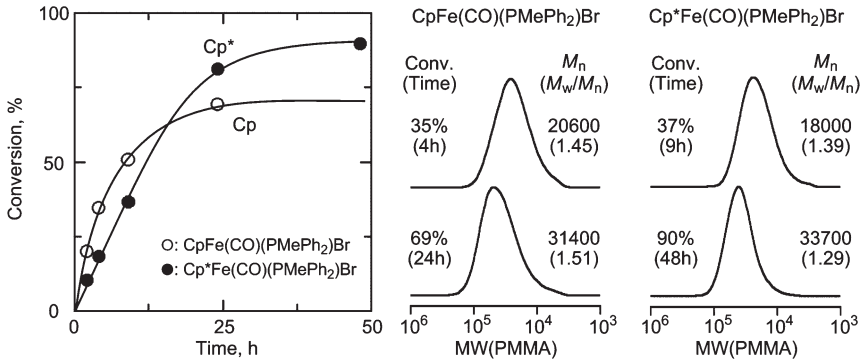


**Figure 6.** Comparisons between CpFe(CO)(PMePh$_2$)Br and Cp*Fe(CO)(PMePh$_2$)Br on living radical polymerization of PEGMA with H−(MMA)$_2$−Br in toluene at 60 °C: [PEGMA]$_0$ = 500 mM; [H−(MMA)$_2$−Br]$_0$ = 5.0 mM; [iron catalyst]$_0$ = 5.0 mM. Iron catalyst: CpFe(CO)(PMePh$_2$)Br (○); Cp*Fe(CO)(PMePh$_2$)Br (●).

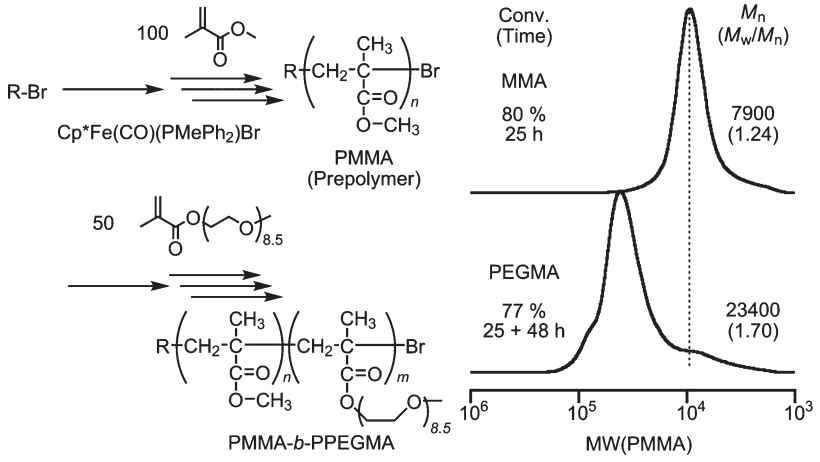


**Figure 7.** SEC curves of PMMA and PMMA-*b*-P(PEGMA) obtained with H−(MMA)$_2$−Br/Cp*Fe(CO)(PMePh$_2$)Br in toluene at 60 °C: [MMA]$_0$ = 2000 mM; [H−(MMA)$_2$−Br]$_0$ = 20 mM; [Cp*Fe(CO)(PMePh$_2$)Br]$_0$ = 5.0 mM; [PEGMA]$_{add}$ = 1000 mM; [Cp*Fe(CO)(PMePh$_2$)Br]$_{add}$ = 2.0 mM.

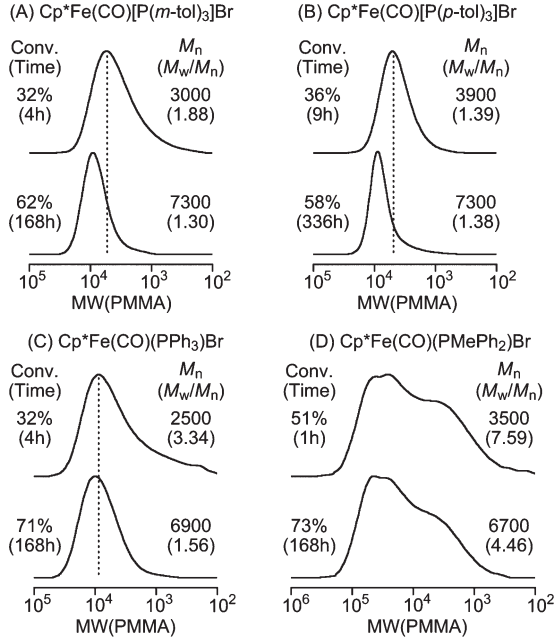


**Figure 8.** Polymerization of MA with H−(MMA)$_2$−Br/Cp*Fe(CO)(L$^{phos}$)Br in toluene at 80 °C: [MA]$_0$ = 4000 mM; [H−(MMA)$_2$−Br]$_0$ = 40 mM; [Cp*Fe(CO)(L$^{phos}$)Br]$_0$ = 10 mM. Cp*Fe(CO)(L$^{phos}$)-Br: (A) Cp*Fe(CO)[P(*m*-tol)$_3$]Br; (B) Cp*Fe(CO)[P(*p*-tol)$_3$]Br; (C) Cp*Fe(CO)(PPh$_3$)Br; (D) Cp*Fe(CO)(PMePh$_2$)Br.

that is effective for MMA ($M_w/M_n \sim 1.3$) is less active and cannot control polymerization of MA ($M_w/M_n > 2$).[23] For MA, the growing radical is inherently reactive, and thus a faster halogen-capping (deactivation) would be particularly significant. Additionally, the less bulky monomer possibly interacts with the catalyst and thereby disrupts the ligand configuration to interfere catalytic performance. From these viewpoints, the Cp*Fe derivatives were promising, relative to the CpFe, because of their lower redox potential and the more bulky structure.

Thus, MA was polymerized with four Cp*Fe(CO)(L$^{phos}$)Br catalysts [L$^{phos}$ = PPh$_3$, PMePh$_2$, P(*m*-tol)$_3$, P(*p*-tol)$_3$] in conjunction with H−(MMA)$_2$−Br in toluene at 80 °C ([MA]$_0$/[initiator]$_0$/[catalyst]$_0$ = 4000/40/10 mM) (Figure 8). With P(*m*-tol)$_3$ and P(*p*-tol)$_3$ ligands, fairly narrow MWDs and molecular weight increase were observed, although the polymerizations markedly slowed down at a limited conversion (~60%) (Figure 8a,b). On the other hand, the PPh$_3$ or PMePh$_2$ complexes gave uncontrolled polymers (Figure 8c, d). These results show that, with bulkier and more electron-donating Cp* and phosphine ligands, Cp*Fe(CO)(L)Br is relatively effective for MA polymerization but that further ligand design might improve its catalytic performance for acrylates.

## Conclusions

A series of heteroligated Cp*Fe(II) complexes with carbonyl and phosphine ligands [Cp*Fe(CO)(L$^{phos}$)Br; L$^{phos}$ = PPh$_3$,

$PMePh_2$, $PMe_2Ph$, P(*m*-tol)$_3$, P(*p*-tol)$_3$] were found to be active catalysts for living radical polymerizations of MMA, MA, and a PEG-functionalized methacrylate (PEGMA). Importantly, the introduction of the Cp* ligand, relative to Cp, allowed a better polymerization control for a functional methacrylate (PEGMA) and acrylate (MA). FT-IR analysis on model reactions revealed a fast carbonyl release that transforms the original 18e complex [Cp*Fe(CO)($L^{phos}$)Br] into an unsaturated 16e form [Cp*Fe($L^{phos}$)Br], most probably acting a true "active" catalyst with a high turnover frequency in the dormant−active equilibrium.

Such an *in situ* transformation of a stable precursor into a true "active" catalyst would be useful for actual applications. We have also tried to prepare the 18e diphosphine Cp* complexes [Cp*Fe($L^{phos}$)$_2$Br], which likely turn into the same 16e intermediate [Cp*Fe($L^{phos}$)Br] during the polymerization. However, they were rather impractical because the starting complexes are too unstable to be isolated. As another way for such an *in situ* generation of the intermediate catalyst, we have found that a direct usage of 18e dicarbonyl iron complex with pentaphenylcyclopentadienyl ligand [($C_5Ph_5$)Fe(CO)$_2$] in the presence of a phosphine ligand was also available for the living radical polymerization. This will be presented in the immediate future.

**Acknowledgment.** This research was partially supported by the Ministry of Education, Science, Sports and Culture, Grant-in-Aid for Creative Scientific Research (18GS0209).

## References and Notes

(1) For recent reviews on transition-metal-catalyzed living radical polymerization, see: (a) Kamigaito, M.; Ando, T.; Sawamoto, M. *Chem. Rev.* **2001**, *101*, 3689–3745. (b) Kamigaito, M.; Ando, T.; Sawamoto, M. *Chem. Rec.* **2004**, *4*, 159–175. (c) Ouchi, M.; Terashima, T.; Sawamoto, M. *Acc. Chem. Res.* **2008**, *41*, 1120–1132. (d) Matyjaszewski, K.; Xja, J. *Chem. Rev.* **2001**, *101*, 2921–2990. (e) *Controlled/Living Radical Polymerization From Synthesis to Materials*; Matyjaszewski, K., Ed.; ACS Symposium Series 944; American Chemical Society: Washington, DC, 2006.

(2) (a) Kato, M.; Kamigaito, M.; Sawamoto, M.; Higashimura, T. *Macromolecules* **1995**, *28*, 1721–1723. (b) Ando, T.; Kato, M.; Kamigaito, M.; Sawamoto, M. *Macromolecules* **1996**, *29*, 1070–1072.

(3) Wang, J. S.; Matyjaszewski, K. *J. Am. Chem. Soc.* **1995**, *117*, 5614–5615.

(4) (a) Bolm, C.; Legros, J.; Paih, J. L.; Zani, L. *Chem. Rev.* **2004**, *104*, 6217–6254. (b) Enthaler, S.; Junge, K.; Beller, M. *Angew. Chem., Int. Ed* **2008**, *47*, 3317–3321.

(5) Ando, T.; Kamigaito, M.; Sawamoto, M. *Macromolecules* **1997**, *30*, 4507–4510.

(6) Matyjaszewski, K.; Wei, M.; Xia, J.; McDermott, N. E. *Macromolecules* **1997**, *30*, 8161–8164.

(7) Kotani, Y.; Kamigaito, M.; Sawamoto, M. *Macromolecules* **1999**, *32*, 6877–6880.

(8) Kotani, Y.; Kamigaito, M.; Sawamoto, M. *Macromolecules* **2000**, *33*, 3543–3549.

(9) Zhu, S.; Yan, D. *Macromolecules* **2000**, *33*, 8233–8238.

(10) Louie, Y.; Grubbs, R. H. *Chem. Commun.* **2000**, 1479–1480.

(11) Göbelt, B.; Matyjaszewski, K. *Macromol. Chem. Phys.* **2000**, *201*, 1619–1624.

(12) Gibson, V. C.; O'Reilly, R. K.; Reed, W.; Wass, D. F.; White, A. J. P.; Williams, D. J. *Chem. Commun.* **2002**, 1850–1851.

(13) O'Reilly, R. K.; Gibson, V. C.; White, A. J. P.; Williams, D. J. *J. Am. Chem. Soc.* **2003**, *125*, 8450–8451.

(14) Xue, Z.; Lee, B. W.; Noh, S. K.; Lyoo, W. S. *Polymer* **2007**, *48*, 4704–4714.

(15) Niibayashi, S.; Hayakawa, H.; Jin, R.-H.; Nagashima, H. *Chem. Commun.* **2007**, 1855–1857.

(16) Uchiike, C.; Terashima, T.; Ouchi, M.; Ando, T.; Kamigaito, M.; Sawamoto, M. *Macromolecules* **2007**, *40*, 8658–8662.

(17) Ferro, R.; Milione, S.; Bertolasi, V.; Capacchione, C.; Grassi, A. *Macromolecules* **2007**, *40*, 8544–8546.

(18) Uchiike, C.; Ouchi, M.; Ando, T.; Kamigaito, M.; Sawamoto, M. *J. Polym. Sci., Part A: Polym. Chem.* **2008**, *46*, 6819–6827.

(19) Ishio, M.; Katsube, M.; Ouchi, M.; Sawamoto, M.; Inoue, Y. *Macromolecules* **2009**, *42*, 188–193.

(20) Takahashi, H.; Ando, T.; Kamigaito, M.; Sawamoto, M. *Macromolecules* **1999**, *32*, 3820–3823.

(21) Watanabe, T.; Ando, T.; Kamigaito, M.; Sawamoto, M. *Macromolecules* **2001**, *34*, 4370–4374.

(22) Ouchi, M.; Ito, M.; Kamemoto, S.; Sawamoto, M. *Chem. Asian J.* **2008**, *3*, 1358–1364.

(23) Ishio, M.; Terashima, T.; Ouchi, M.; Sawamoto, M. *Polym. J.*, submitted.

(24) Ando, T.; Kamigaito, M.; Sawamoto, M. *Macromolecules* **2000**, *33*, 5825–5829.

(25) Barras, J.-P.; Davis, S. G.; Metzler, M. R.; Edwards, A. J.; Humphreys, V. M.; Prout, K. *J. Organomet. Chem.* **1993**, *461*, 157–165.

(26) Ando, T.; Kamigaito, M.; Sawamoto, M. *Tetrahedron* **1997**, *53*, 15445–15457.

(27) (a) Fischer, E. O.; Moser, E. *Inorg. Synth.* **1970**, *12*, 35–36. (b) Hallam, B. F.; Pauson, P. L. *J. Chem. Soc.* **1956**, 3030–3037.

(28) Treichel, P. H.; Shubkin, R. L.; Barnett, K. W.; Reichard, D. *Inorg. Chem.* **1966**, *5*, 1177–1181.

(29) King, R. B.; Stone, F. G. *Inorg. Synth.* **1963**, *7*, 99–115.